EYE-CLIMA
Verifying emissions of climate forcers

Updated input driving datasets for process-based models

DELIVERABLE 2.2

Author(s):	Philippe Peylin, Tuula Aalto, Vladislav Bastrikov, Tiina Markkanen, Antti Leppänen, Almut Arneth, Jianyong Ma

Date of submission:	17-04-2025
Version:	1
Responsible partner:	CNRS-LSCE
Deliverable due date:	31-08-2024
Dissemination level:	Public

Call:	HORIZON-CL5-2022-D1-02
Topic:	Climate Sciences and Responses
Project Type:	Research and Innovation Action
Lead Beneficiary:	NILU - Norsk Institutt for Luftforskning

This project has received funding from the European Union's Horizon Europe research and innovation programme under grant agreement No 101081395

Document History

Version	Date	Comment	Modifications made by
0.1	07-04-2025	First Draft	Philippe Peylin, Tuula Aalto, Tiina Markkanen, Antti Leppänen, Almut Arneth, Jianyong Ma, Vladislav Bastrikov, Sebastiaan Luyssaert
0.2	08-04-2025	Internal review	Maria Tenkanen
1.0	17-04-2025	Submitted to the Commission	Rona Thompson

This project has received funding from the European Union's Horizon Europe research and innovation programme under grant agreement No 101081395

Summary

To simulate carbon dioxide (CO_2), methane (CH_4) and nitrous oxide (N_2O) fluxes across Europe using the selected process-based models (ORCHIDEE, LPJ-GUESS and JSBACH), input datasets and additional data are required. These datasets are needed either to calibrate key model parameters or to validate the simulated fluxes. This deliverable thus consists of the description of the collected data for this modelling effort. Apart from the climate data, it is mostly a collection of existing datasets derived during related projects and community efforts rather than the processing of specific raw data. The main input datasets gathered are:

- Climate data that correspond to the ERA5-land reanalysis from ECMWF (at 11 km resolution) further bias corrected using the CRU monthly data. The product was first derived during the VERIFY project and has been extended in EYE-CLIMA to cover recent years (up to 2023).
- A European subset of the HILDA+ (HIstoric Land Dynamics Assessment+) dataset on land use/land cover (LULC) change. HILDA+ is a global dataset starting in 1960 at 1 km spatial resolution, integrating multiple open data streams (from high-resolution remote sensing, long-term land use reconstructions and statistics).
- Soil organic carbon stocks from the SoilGrids database used in ORCHIDEE to initialise the model soil C content. For soil physical properties, we will try to use the Land Use and Cover Area frame Statistical survey (LUCAS) topsoil data, although currently, the LPJ model uses the WISE dataset.
- Cropland management datasets: the MIRCA2000 global dataset with a spatial resolution of 0.083° will be used to provide both irrigated and rain-fed crop harvest areas for all major food crops. For reconstructing the history of anthropogenic nitrogen inputs to the terrestrial biosphere, a comprehensive and synthetic dataset from Tian et al. (2022) will be used.
- Grassland management datasets are still being gathered by the modelling groups in order to derive spatial and temporal information about cutting and grazing. For this, livestock density distribution maps for different livestock categories are key and they will be taken from the Gridded Livestock of the World dataset (GLW2; Robinson et al., 2014).
- Forest management and evaluation datasets: different datasets assembled in previous projects, based on National Forest Inventory (NFI) data and remote sensing data, have been gathered to calibrate and evaluate the forest demography of ORCHIDEE and LPJ-GUESS. Recent dataset for Europe from Pucher et al. (2022) are also being used (especially forest age classes and forest height).

The EYE-CLIMA model input datasets are, however, a living structure, growing out of a collaboration between the three modelling groups. As such, the collection of data and this document will continue to be updated as user needs evolve.

This project has received funding from the European Union's Horizon Europe research and innovation programme under grant agreement No 101081395

TABLE OF CONTENTS

This project has received funding from the European Union's Horizon Europe research and innovation programme under grant agreement No 101081395

1. Introduction

For the quantification of greenhouse gas (GHG) surface fluxes within the EYE-CLIMA project, three process-based land surface models are going to play a central role. They integrate our physical understanding of the land surface processes controlling these fluxes and are used to extrapolate and interpolate knowledge, obtained from measurements and theory, spatially and temporally. The application of models requires, however, numerous datasets to parameterise the models and validate the results. Climate, soil, management (for cropland, forest and grassland) and land use/land cover are the main driving data that are required for modelling the carbon and nitrogen dynamics (namely CO_2, CH_4 and N_2O fluxes). Therefore, the first aim of WP2 (Task 2.1) was to collect these data and provide them to the other tasks of WP2. The collection includes data needed to perform the simulations but also to improve and validate model outputs.

A first version of the input dataset was provided earlier in the project with the deliverable D2.1 (First input driving datasets for process-based models). The current deliverable provides an update of the collected data that defines the final version of the input dataset. As such it thus includes not only the description of the updated datasets, but it also recalls the description of the first input datasets.

This project has received funding from the European Union's Horizon Europe research and innovation programme under grant agreement No 101081395

2. Meteorological forcing dataset

Two input datasets were considered as potential meteorological forcing for the process-based models used in the EYE-CLIMA project:

- A product based on the ERA5-land climate reanalysis of ECMWF (European Center for Medium-Range Weather Forecast) with an additional bias correction, at the spatial resolution of around 11 km.
- A new reanalysis produced also by ECMWF specifically for Europe: the Copernicus Regional Reanalysis for Europe (CERRA), at the spatial resolution of 5.5 km: https://climate.copernicus.eu/copernicus-regional-reanalysis-europe-cerra.

Given that the CERRA product only starts in 1983 (which is sub-optimal to run the model over the historical period for CO_2) and that some preliminary analyses showed precipitation biases at some sites, we decided for the first round of simulations of EYE-CLIMA to use the ERA5-land bias corrected product. For the second round, we chose to keep using it, because the CERRA product will only be extended backward in time during 2025 (see the above website for CERRA).

The ERA5-land bias corrected product was first produced in the VERIFY project and further extended in the CoCO2 project. In 2020, the VERIFY project, through the combined efforts of the University of East Anglia, ECMWF, and LSCE, processed high-resolution meteorological forcing data from the ERA5-Land dataset at 3-hourly resolution across Europe for the historical period: 1901 to 2019. The ERA5-Land has an operational status that guarantees that data for the previous year will be available by April/May of the current year.

The ERA5-Land reanalysis was then re-aligned with the CRU observational time series dataset. The CRU TS dataset was developed and has been subsequently updated, improved and maintained with support from a number of funders, principally the UK's Natural Environment Research Council (NERC) and the US Department of Energy. This procedure changes the monthly means of each 0.5° pixel to match that of CRU observations; consequently, the regional monthly-averaged climate is that of the CRU, while the sub-monthly and higher spatial resolution come from ERA5-Land. During the CoCO2 project, such a dataset was extended to the year 2021. Within EYE-CLIMA, we have re-aligned the whole time series (from 1901 onwards) and not only the last year, 2023. The CRU dataset was recently updated to V4.08 on the 27 June 2024, a release that covers the period 1901-2023. More information on the new CRU version can be found at:

https://crudata.uea.ac.uk/cru/data/hrg/cru_ts_4.07/Release_Notes_CRU_TS_4.07.txt

The re-aligned dataset is available from the VERIFY THREDDS server:

https://verifydb.lsce.ipsl.fr/thredds/verify/VERIFY_INPUT/CRUERA_V4.0/catalog.html

The most complete set of meteorological forcing are available at sub-daily (3-hourly) time steps but also some variables are available at daily and monthly time steps. The list of available variables is provided in the table below. To access the THREDDS server, you need a login with a username and password:

Username: vdbuser

Password: V3r1fy

(Note that several other European projects have asked the permission to use this dataset.)

In order to illustrate some features of this dataset, we provide below two figures for the annual mean and July mean of the surface air temperature (Figure 1) and the precipitation (Figure 2) comparing the last two years of the dataset (2022 and 2023). For the temperature, we see that the year 2023 was on

This project has received funding from the European Union's Horizon Europe research and innovation programme under grant agreement No 101081395

average similar to 2022 with a mean temperature across the European domain of 8.88°C for 2023 and 8.75°C for 2022. For July, year 2022 was slightly warmer than July 2023 (19.6°C for 2022 and 19.0°C for 2023). For the precipitation, the annual mean was higher in 2023 than in 2022 (2.1 vs 1.8 mm/day). This was also the case in July.

Table 1: *List of the variables and time steps in the dataset.*

Variable	3-hourly	Daily	Monthly
Tair	X	X	X
Tmax	X	X	
Tmin	X	X	
Wind_N & Wind_E	X	X	
WS	X	X	
Psurf	X	X	
LWdown	X	X	
SWdown	X	X	X
Qair	X	X	
Rainf	X		
Snowf	X		
Precipitation	X	X	X
RH	X	X	

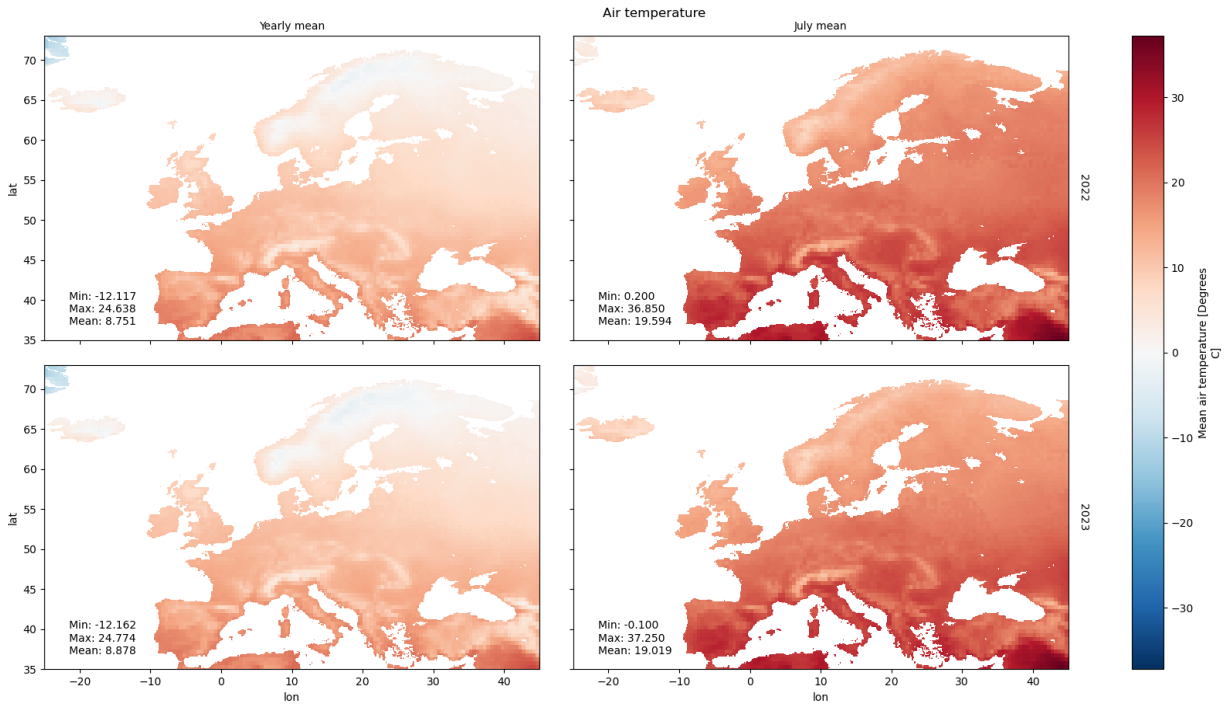

Figure 1*: Illustration of the surface temperature forcing used within EYE-CLIMA (derived from ERA5-Land with CRU monthly bias correction) for two years, 2022 (top) and 2023 (bottom) over Europe. The left column shows the annual mean and the right column the July mean.*

This project has received funding from the European Union's Horizon Europe research and innovation programme under grant agreement No 101081395

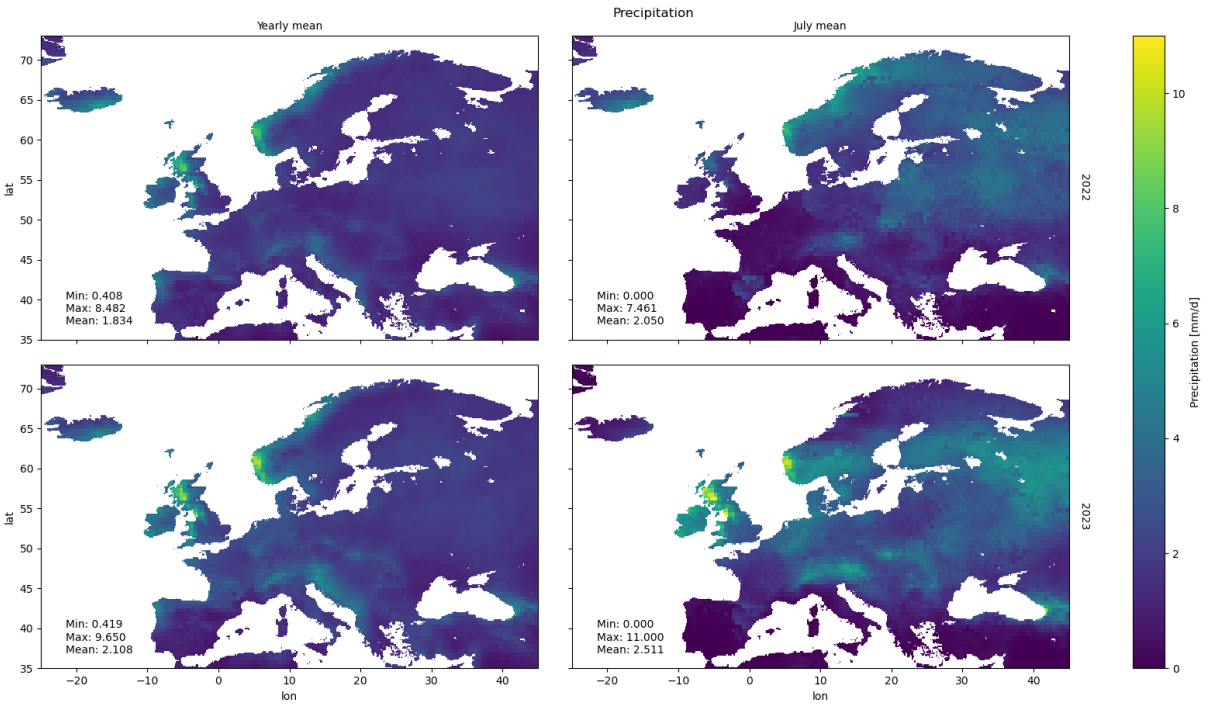

***Figure 2**: Illustration of the precipitation forcing used within EYE-CLIMA (derived from ERA5-Land with CRU monthly bias correction) for two years, 2022 (top) and 2023 (bottom) over Europe. The left column shows the annual mean and the right column the July mean.*

3. High-resolution land cover and land use data

3.1 HILDA+ land use/cover dataset

We proposed to use a European subset of the HILDA+ (HIstoric Land Dynamics Assessment+) global dataset on land use/land cover (LULC) change (Winkler et al., 2020). HILDA+ is a global dataset of land use/cover change starting in 1960 at 1 km spatial resolution and annual temporal resolution. It is based on a data-driven reconstruction approach and integrates multiple open data streams (from high-resolution remote sensing, long-term land use reconstructions and statistics). It covers six generic land use/cover categories: 1: Urban areas, 2: Cropland, 3: Pasture/rangeland, 4: Forest, 5: Unmanaged grass/shrubland, 6: Sparse/no vegetation. Forest generic type is further refined into different plant functional types (see Figure 3).

Starting with a FAO-calibrated base map (derived from ESA Copernicus LC100 2015), HILDA+ allocates land use/land cover transitions iteratively for each time step (annually) and for each country along a backwards-looking time loop on a 1×1 km grid. Net change magnitudes are based on national FAO land use and population statistics. Gross change magnitudes are calculated from mean transition matrices, which are extracted from a time series of satellite-derived land use/land cover maps. The change allocation depends on class probability maps (mean class fractions) generated from year- and region-specific remote sensing-based land use/land cover maps.

The data was not updated since the first report and the product thus only covers up to 2020. For the following years (up to 2023), we use the land cover distribution of 2020.

This project has received funding from the European Union's Horizon Europe research and innovation programme under grant agreement No 101081395

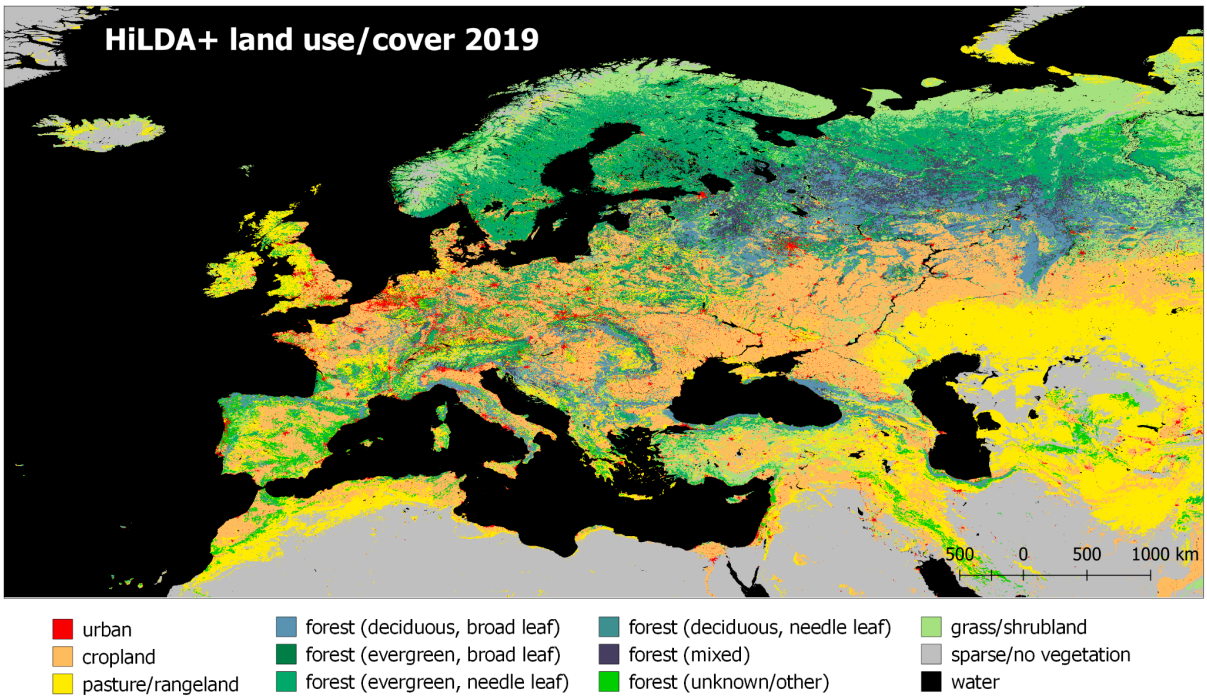

***Figure 3**: Land use/cover from HILDA+ to be used within EYE-CLIMA.*

3.2 Mapping HILDA+ to ORCHIDEE Plant Functional Types

From the HILDA+ product, we had to map the generic land cover into the specific Plant Functional Types (15 PFTs) of the ORCHIDEE land surface model. The approach consists of defining a cross-walking table (CWT) between the generic land use/land cover classes of HILDA+ and the 15 PFTs of ORCHIDEE, using also additional information such as: i) a climate zone definition from Köppen-Geiger, ii) the C4 grassland fraction from Still et al. (2019) and the C4 crop fraction from LUH2 historical dataset. The figure below illustrates how such CWT is defined with the "Still" and "LUH2" additional maps.

The process with the different maps that are used as well as the resulting PFTs is illustrated on a dedicated webpage of the ORCHIDEE model development:

https://orchidas.lsce.ipsl.fr/dev/verify/hilda.php

KG CLASS	11 Urban	22 Cropland	33 Pasture	40 Forest Unknown/Other	41 Forest EvNe	42 Forest EvBr	43 Forest DeNe	44 Forest DeBr	45 Forest Mixed	55 Grass/shrubland	66 Other land	77 Water	0 No data
Tropical	80% → PFT1 20% → PFT14	PFT12/13 (using LUH2)	PFT14/11 (using Still)	50% → PFT2 50% → PFT3	PFT2	PFT2	PFT3	PFT3	50% → PFT2 50% → PFT3	40% → PFT2 40% → PFT3 20% → PFT14/11 (using Still)	PFT1	PFT1	masked at ocean dillute between given PFTs at coast
Arid Warm	80% → PFT1 20% → PFT10		PFT10/11 using Still	33% → PFT4 33% → PFT5 34% → PFT6	PFT4	PFT5	PFT6	PFT6	33% → PFT4 33% → PFT5 34% → PFT6	26% → PFT4 27% → PFT5 27% → PFT6 20% → PFT10/11 (using Still)			
Arid Cool													
Temperate Warm													
Temperate Cool													
Boreal Warm	80% → PFT1 20% → PFT15		PFT15/11 (using Still)	33% → PFT7 33% → PFT8 34% → PFT9	PFT7	PFT7	PFT9	PFT8	33% → PFT7 33% → PFT8 34% → PFT9	26% → PFT7 27% → PFT8 27% → PFT9 20% → PFT15/11 (using Still)			
Boreal Cool													

***Figure 4**: Cross-walking table from HILDA+ classes to ORCHIDEE PFTs.*

The figure 5 illustrates the spatial distribution and temporal evolution of one PFT of ORCHIDEE (Temperate Broadleaf Summer-green forest, PFT6) following the use of HILDA+ classes. We notice a significant increase in this forest PFT at the expense of crops and natural grassland.

This project has received funding from the European Union's Horizon Europe research and innovation programme under grant agreement No 101081395

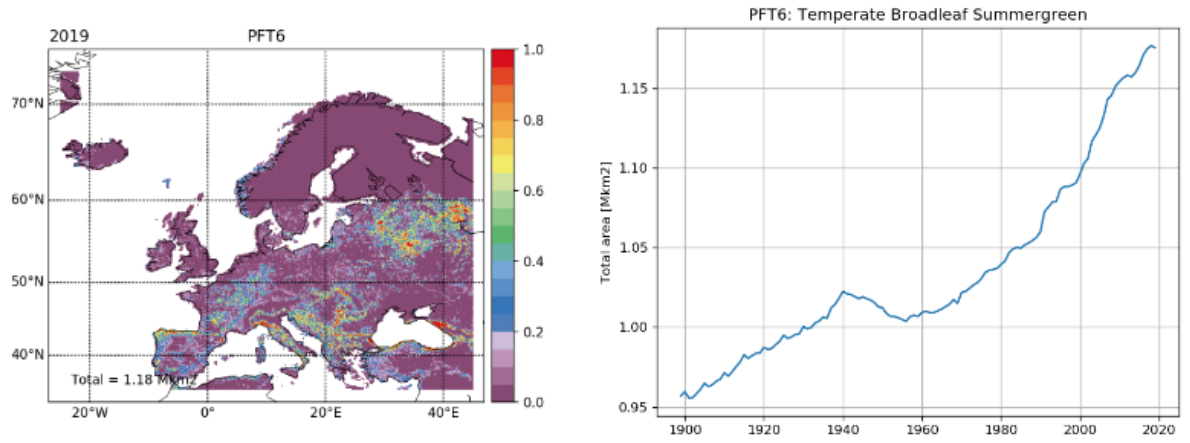

***Figure 5**: Spatial distribution and temporal evolution of the Temperate Broadleaf Summer-green forest (PFT6) of ORCHIDEE following the use of the HILDA+ land use/land cover classes and the cross-walking approach defined above.*

3.3 Mapping HILDA+ to LPJ-GUESS Plant Functional Types

The LULC information required in LPJ-GUESS primarily includes four vegetation types: cropland, pasture, managed forest, and natural vegetation. To align with this classification, we aggregated the unmanaged forest and unmanaged grass/shrubland from the HILDA+ data set (Winkler et al., 2020) into the "natural vegetation" category in LPJ-GUESS, and regridded it from 0.01° to 0.125° resolution across Europe. Likewise, the other forest, pasture/rangeland, and cropland classes in HILDA+ were aggregated to "managed forest", "pasture" and "cropland" categories, respectively, at the same resolution (Table 2).

To initialize the timing of clear-cutting across tree species in managed forests, we used the European forest age data set from Pucher et al. (2022). Since Pucher et al. (2022) describe some forest ages ranging between 100 and 140 years, the aggregated LULC data from HILDA+ was further extended back to 1870 to ensure consistency. Figure 6 below illustrates the spatial distribution and time series of the four vegetation types after processing HILDA+ and forest age data at 0.125° resolution. In 2020, cropland was the dominant vegetation type in Europe, covering an estimated 242 Mha, followed by natural vegetation (224 Mha), managed forest (210 Mha), and pasture (105 Mha).

***Table 2**: Categorizing land use/cover from HILDA+ to LPJ-GUESS at 0.125° resolution*

Land use/cover categories in HILDA+ (from)	**Land use/cover categories in LPJ-GUESS (to)**
Urban	Urban
Cropland	Cropland
Pasture/Rangeland	Pasture
Evergreen needle leaf forest (unmanaged)	Natural Vegetation
Evergreen broad leaf forest (unmanaged)	
Deciduous needle leaf forest (unmanaged)	
Deciduous broad leaf forest (unmanaged)	
Mixed forest (unmanaged)	
Grass/Shrubland (unmanaged)	
Other forest (managed)	Managed forest
Sparse/no vegetation	Barren
Water	N/A

This project has received funding from the European Union's Horizon Europe research and innovation programme under grant agreement No 101081395

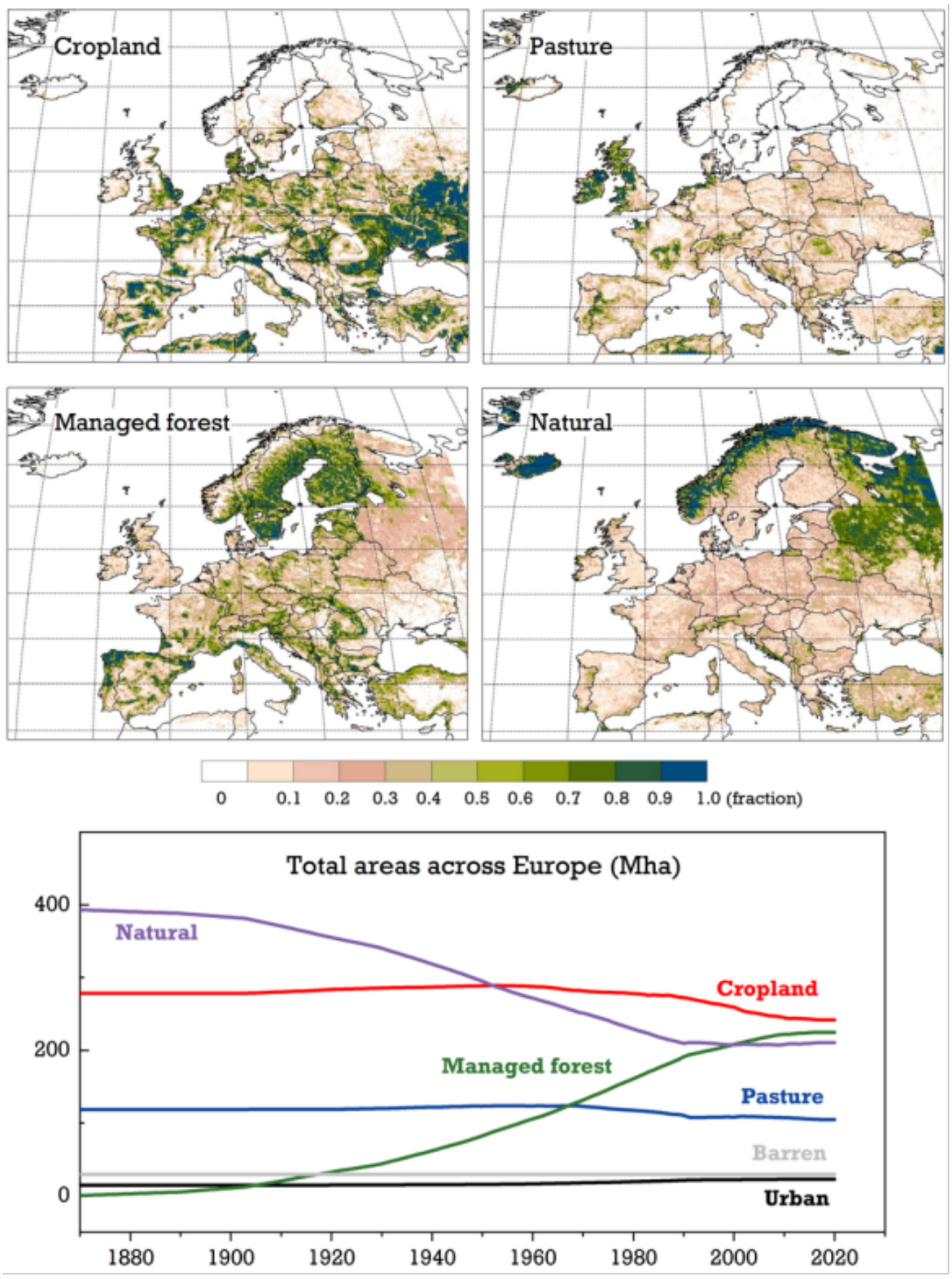

***Figure 6**: Maps of land use/cover fractions of the remapped HILDA+ data sets in LPJ-GUESS (averaged over 2011-2020), and total areas in each land use/cover class across Europe from 1870-2020.*

3.3 Mapping HILDA+ to JSBACH Plant Functional Types

We mapped HILDA+ types into JSBACH's non-peatland plant functional types (PFTs) according to Figure 7. The status of HILDA+ in 2020 was used to represent the current-day non-peatland PFT distribution. The target JSBACH PFTs are given in Table 3. The main deviations from ORCHIDEE's respective mapping (Figure 4) are the cross-walkings of HILDA+ classes 40 and 45 at the Boreal zone where the classes are divided into two classes instead of three. The other main deviation is the HILDA+ class "Other land" that

This project has received funding from the European Union's Horizon Europe research and innovation programme under grant agreement No 101081395

contributed to the "area inhabitable for vegetation" in JSBACH that comprises a complement of maximum vegetation ratio (veg_ratio_max).

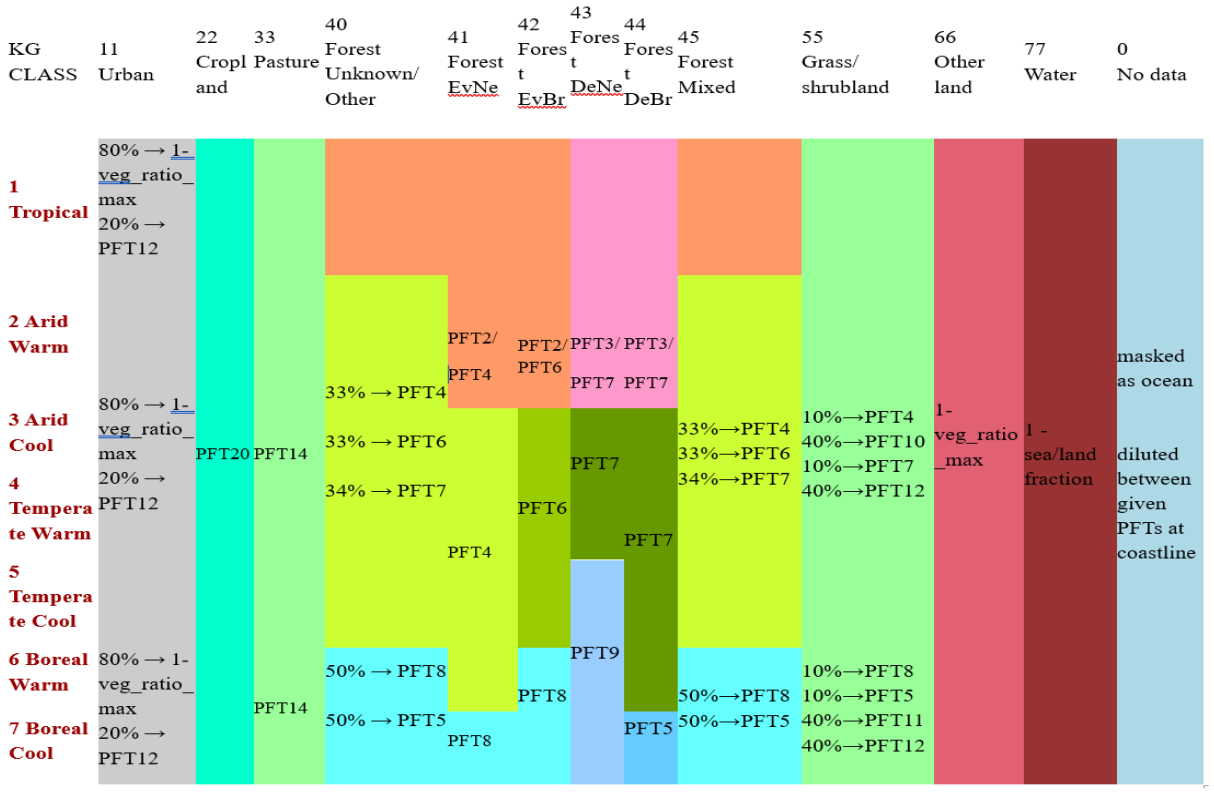

Figure 7*. Mapping of HILDA+ -types to JSBACH PFTs. Overall, the classes are divided into PFT combinations according to the climate zone definition from Köppen-Geiger.*

Table 3*. Plant functional types in JSBACH-HIMMELI*

1: Glacier	12: C3 grass
2: Tropical evergreen trees	13: C4 grass
3: Tropical deciduous trees	14: Pasture
4: Extra-tropical evergreen trees	15: C3 pasture
5: Extra-tropical deciduous trees	16: C4 pasture
6: Temperate broadleaf evergreen trees	17: Tundra
7: Temperate broadleaf deciduous trees	18: Swamp
8: Coniferous evergreen trees	19: Crops
9: Coniferous deciduous trees	20: C3 crop
10: Raingreen shrubs	21: C4 crop
11: Deciduous shrubs	22: Peatland

3.4 Wetland spatial and temporal extent

For the circumpolar current-day wetland extent in JSBACH-HIMMELI, we used GLWD.v2 (Lehner et al., 2024) wetland classes Arctic/boreal non-forested peatland, Temperate non-forested peatland and Tropical non-forested peatland (class numbers 23, 25 and 27, respectively).

This project has received funding from the European Union's Horizon Europe research and innovation programme under grant agreement No 101081395

For the European areal coverage of the EU-CORINE land cover (CLC, https://land.copernicus.eu/en/products/corine-land-cover), the CLC classes “bogs” and “inland marshes” are interpreted as wetland.

For Finland, where intense drainage of pristine peatlands for forestry and agriculture took place during the 20th century, we used the detailed data from GTK (Geological Survey of Finland, https://tupa.gtk.fi/paikkatieto/meta/suotyypit_ja_turvekankaat.html), which was recently published (2023) and contains remaining peat stocks both in managed and pristine peatlands. The land cover classes are detailed by various, mainly plant species distribution based, peatland type characteristics and state of drainage and current land use. We identified the classes which correspond to pristine peatlands by vegetation and wetness, and applied those as wetlands in JSBACH-HIMMELI (Figure 8). With this classification the wetland area in Finland is about 27 000 km², while according to Corine it is about 24 000 km².

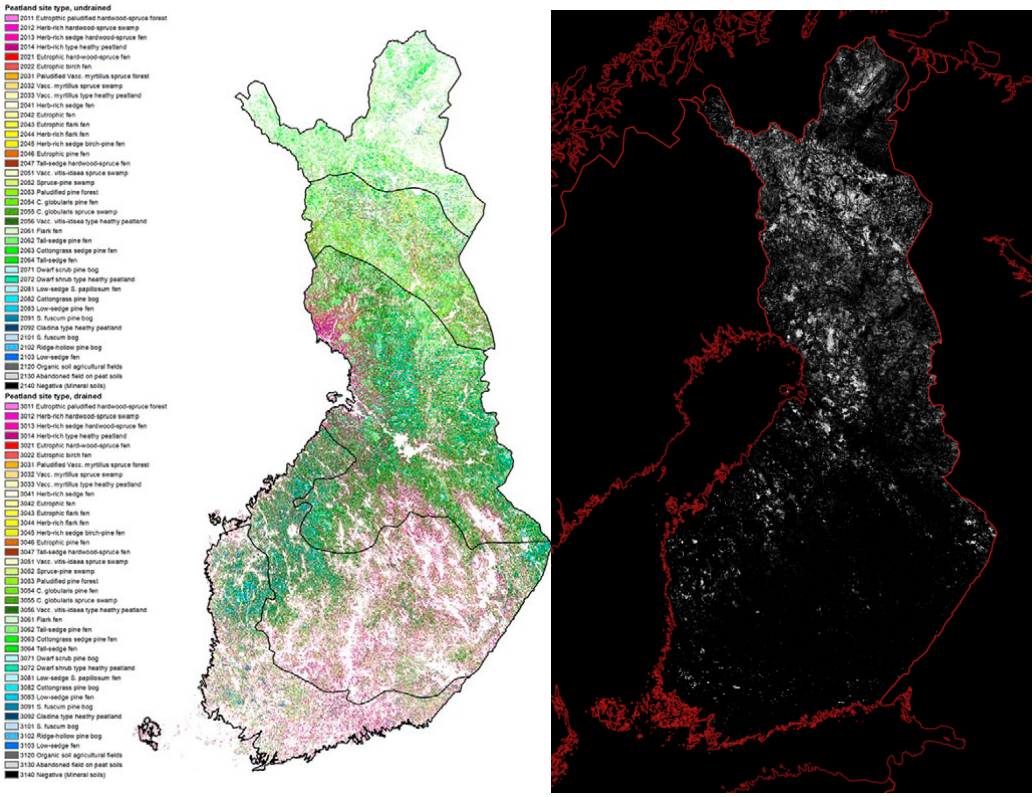

***Figure 8**. Left: Managed and pristine peatland land cover types in Finland (figure adopted from Ministry of Environment, Report 2023:33) and Right: Peatland land cover types interpreted as wetlands by FMI.*

The wetland fraction composite was first mapped to the target grid. Secondly, the grid cell specific wetland fractions were subtracted from the non-wetland JSBACH PFTs in the following order: C3 grass, Raingreen shrubs/Deciduous shrubs, Extra-tropical evergreen trees/Coniferous evergreen trees, Temperate broadleaf deciduous trees and Pasture. If the fractional coverage of wetlands exceeded the fraction of C3 grass in the grid-cell the remainder was subtracted from the respective shrubs PFT and so on. The reasoning behind the order of the subtraction, is that the relatively open and treeless mires likely originally got mapped to the most open Grass/Shrubland class in HILDA+.

In addition to the constant fractional distribution of wetlands on peat soils, we use the monthly inundation fraction data WAD2M version 2.0 (Zhang et al., 2021) to simulate methane emissions from inundated

This project has received funding from the European Union’s Horizon Europe research and innovation programme under grant agreement No 101081395

soils. The areal fraction of wetlands on peat soils (as defined above) in each grid cell is first subtracted from the monthly inundated fraction and the remainder is assigned as inundated soil fraction. The land area after removing the wetlands on peat soils and the varying inundated fraction have been assigned for upland mineral soils.

4. Soil organic carbon stocks and soil properties

4.1 Soil properties

Although the three models (ORCHIDEE, LPJ-GUESS and JSBACH) are using different soil properties datasets in their current settings, we will try to harmonise them in the course of the project towards the use of a common dataset. We will use the topsoil physical properties for Europe based on the Land Use and Cover Area frame Statistical survey (LUCAS) topsoil data. These data are downloaded from the following website: https://esdac.jrc.ec.europa.eu/.

LUCAS aimed at collecting harmonised data about the state of land use/cover over the European Union (EU). Among these 200k land use/cover observations selected for validation, a topsoil survey was conducted at about 10% of these sites. Topsoil sampling locations were selected to be representative of the European landscape using a Latin hypercube stratified random sampling, considering CORINE land cover 2000, the Shuttle Radar Topography Mission (SRTM) DEM and its derived slope, aspect and curvature. Several soil properties were predicted using hybrid approaches like regression kriging. For those datasets, topsoil texture and related derived physical properties were predicted. Regression models were fitted using, along with other variables, remotely sensed data coming from the MODIS sensor. The high temporal resolution of MODIS allowed the detection of changes in the vegetative response due to soil properties, which can then be used to map soil feature distribution. The prediction of intrinsically co-linear variables like soil texture required the use of models capable of dealing with multivariate constrained dependent variables like Multivariate Adaptive Regression Splines (MARS). Cross-validation of the fitted models showed that the LUCAS dataset constitutes a good sample for mapping purposes leading to cross-validation R2 between 0.47 and 0.50 for soil texture and normalised errors between 4 and 10%.

This dataset provides the following soil properties at 500 m resolution, for the geographical coverage: European Union (EU) plus Balkan countries, Switzerland and Norway:

- Clay content (%) in topsoil (0-20cm) modelled by Multivariate Additive Regression Splines
- Silt content (%) in topsoil modelled by Multivariate Additive Regression Splines
- Sand content (%) in topsoil modelled by Multivariate Additive Regression Splines
- Coarse fragments (%) content in topsoil modelled by Multivariate Additive Regression Splines
- Bulk density derived from soil texture datasets (obtained from the packing density and the mapped clay content following the equation of Jones et al., 2003)

With the ORCHIDEE model, although we are using the global USDA soil texture map as the standard, a test with the LUCAS dataset will be made to see the impact of different soil properties on the soil water holding capacity and consequently on the different GHG fluxes.

For the LPJ–GUESS model, soil physical property data sets are the same as those used in the first round of simulations.

This project has received funding from the European Union's Horizon Europe research and innovation programme under grant agreement No 101081395

In addition to the plant functional types, the HILDA+ classification guided the attribution of a subset of surface parameters in JSBACH-HIMMELI. For that aim, HILDA+ classes were linked to USGGD land cover classes (Table 4).

***Table 4**. Linking HILDA+ to USGGD land cover classes*

HILDA+ land cover class	USGGD land cover class
11 Urban	47 Dry Woody Scrub
22 Cropland	94 Crops, Grass, Shrubs
33 Pasture	56 Forest and Field
40 Forest Unknown/Other	24 Mixed Forest
41 Forest EvNe	21 Conifer Boreal Forest
42 Forest EvBr	6 Evergreen Broadleaf Forests
43 Forest DeNe	4 Deciduous Conifer Forest
44 Forest DeBr	5 Deciduous Broadleaf Forest
45 Forest Mixed	24 Mixed Forest
55 Grass/shrubland	40 Cool Grasses and Shrubs
66 Other land	8 Bare Desert

The attribution of parameter values to the USGGD classes is given in Hagemann et al. (2002; http://hdl.handle.net/11858/00-001M-0000-002B-539B-6). For soils, we used Tanneberger et al. (2017) peatland extent data to adjust soil parameter values to account for the peat fraction within each grid cell. For the land area beyond the coverage of the Tanneberger et al. (2017) peatland map, we used HWSD2 (Harmonized World Soil Database v2, FAO & IIASA, 2023) peatland extent. Parameters from Hagemann and Stacke (2015) were used to describe the soil properties, e.g. soil porosity, saturated hydraulic conductivity, field capacity and wilting point and saturated moisture potential. However, to mitigate the impact of peat soil properties to the overall soil moisture modelling, instead of using only peatsoil parameter values, we used the average values of Peatsoil and Loamy Sand classes for peatland fractions of each grid-cell. Moreover, the soil parameters of Loamy Sand from Hagemann and Stacke (2015) were used for all non-peat soil fractions.

4.2 Soil organic carbon stocks

With the ORCHIDEE model, we use the SoilGrids database (see https://www.isric.org/explore/soilgrids; Ribeiro and Batjes (2019) ; Poggio et al. (2021)) to initialise the model soil organic carbon content (and its vertical distribution) and then we let the model equilibrate with a long spin-up simulation of thousands of years, recycling a 10-year climate forcing. Figure 9 illustrates the soil organic carbon content for the upper 30 cm of soil as estimated by the SoilGrids product. Note that we also have optimised key soil organic matter decomposition parameters from the CENTURY module (used in ORCHIDEE) so that the SOC content after the spin-up remains close to that of the SoilGrids database. This SOC content is also used to weigh soil dry and solid thermal conductivities, thermal capacity and to correct the value of the porosity used to calculate the saturated conductivity and the saturation ratio. With ORCHIDEE, the SoilGrids data are thus used both for the initialisation and the evaluation after the spin-up.

This project has received funding from the European Union's Horizon Europe research and innovation programme under grant agreement No 101081395

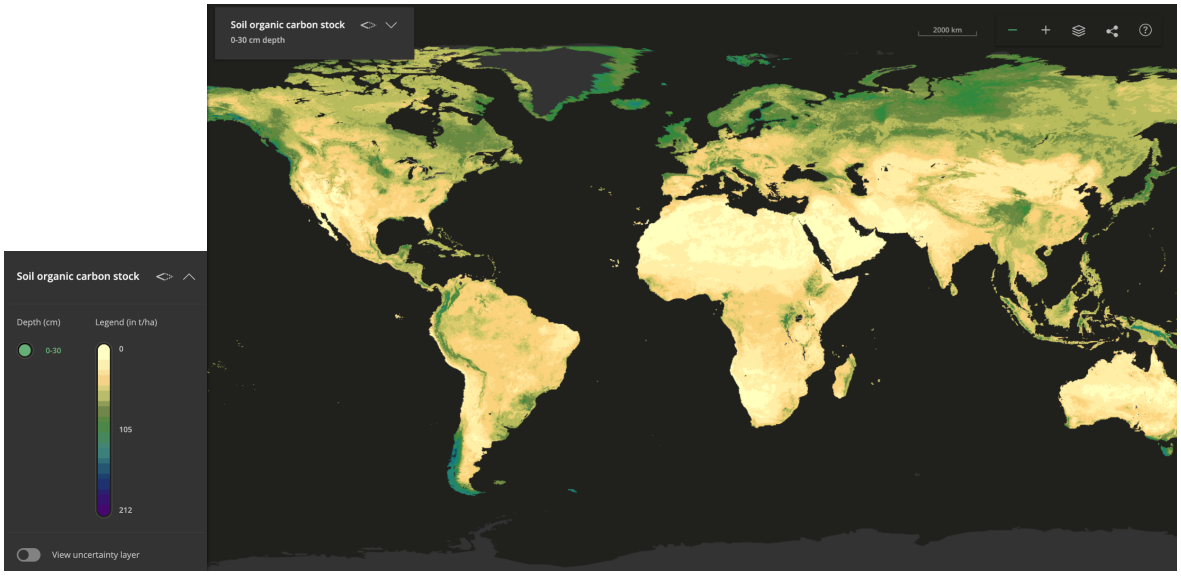

***Figure 9**: Maps of soil organic carbon stock (in t/ha) from the SoilGrids dataset.*

With the JSBACH model, soil organic carbon stocks were accumulated in a long spin-up simulation of three thousand years, using as an input a period of climate drivers in a loop, and corresponding simulation of NPP and water table levels. The peat accumulation is a continuous process in water-logged conditions, and thus the simulation was not attempted to run until equilibrium, rather the simulation was ended when peat depths reach current-day levels.

Like the JSBACH model, soil organic carbon stock in LPJ-GUESS was computed as the long-term accumulation under the potential natural vegetation with a 1000-year spin-up simulation.

5. Cropland management datasets

For LPJ-GUESS, the cropland data sets are the same as those used in the first round of simulation with thus no specific updates. These datasets will also be used with the ORCHIDEE model as much as possible. Currently, the ORCHIDEE model team is integrating the cropland specificities developed in a separate branch, ORCHIDEE-CROP (Wu et al., 2016) into the main version of the model that includes the nitrogen cycle and that will be used to simulate the three GHG fluxes. The first set of ORCHIDEE simulations for EYE-CLIMA was made with a version that only accounts for generic C3 and C4 crops and thus using the FAO dataset (FAOSTAT, 2023) for the spatial distribution of these two “photosynthetic-pathways” of crops. Unfortunately, the second round of simulation with ORCHIDEE will still be based on the generic crops as the version with specific crops is not fully optimized and operational yet. However, before the end of the project, ORCHIDEE will use, like LPJ-GUESS, major crop functional types for Europe and thus use the datasets described below (also described in the first version of the input dataset deliverable).

5.1 Crop growth distribution dataset

MIRCA2000 (Portmann et al., 2010) is a global dataset with a spatial resolution of 5 arc minutes (=0.083°) which provides both irrigated and rain-fed crop harvest areas of 26 crop classes around the year 2000. The dataset includes all major food crops (wheat, maize, rice, barley, rye, millet, sorghum, soybean, sunflower, potato, cassava, sugarcane, sugar beet, oil palm, canola, groundnut, pulses, citrus, date palm, grape, cocoa, coffee, other perennials, fodder grasses, other annuals) as well as cotton.

This project has received funding from the European Union’s Horizon Europe research and innovation programme under grant agreement No 101081395

At present, cropland in LPJ-GUESS is characterised by six crop functional types (CFTs): two temperate C3 crops with spring and autumn sowing dates, a tropical C3 crop representing rice, a C4 crop representing maize, and two N-fixing grain legumes representing soybean and pulses. Considering the importance of barley, pulses (e.g., beans and peas), rapeseed, and maize in the overall agriculture in Europe (e.g., harvest areas and total production; FAOSTAT, 2023), we thus aggregated these main food crops from MIRCA2000 to CFTs in LPJ-GUESS from 0.083° to 0.125° resolution for better accounting for agricultural production in this region. The details on how we mapped the MIRCA2000 crops to the LPJ-GUESS CFTs are given in Table 5 and Figure 10 below.

Our estimated total areas of six CFTs in Europe are in general higher than the statistics from FAO (Figure 11), most likely due to the inclusion of parts of areas in Turkey and Russia across the European domain in our estimation (Figure 10). The overestimation is expected to be largely diminished when these two countries are removed from the comparison.

Table 5: *Categorizing crop types from MIRCA2000 to LPJ-GUESS at 0.125° resolution*

Crop classes in MIRCA2000 (from)	**Crop functional types (CFTs) in LPJ-GUESS (to)**
Potatoes, Sugar beet, Sunflowers	C3 crops sown in spring (representing spring wheat)
Barley, Rapeseed, Rye, Wheat	C3 crops sown in autumn (representing winter wheat)
Maize, Millet, Sorghum	C4 crops (representing maize)
Rice	Rice
Soybean	Soybean
Pulses	Pulses (representing faba bean)
Others (e.g., Groundnut, Oil palm, Sugarcane, Date palm, Citrus, Cocoa, Coffee, Cassava)	N/A

5.2 Nitrogen fertilisation dataset

Tian et al. (2022) developed a comprehensive and synthetic dataset for reconstructing the History of anthropogenic Nitrogen inputs (HaNi) to the terrestrial biosphere. The HaNi dataset takes advantage of different data sources in a spatiotemporally consistent way to generate a set of gridded high-resolution N input products from the preindustrial period to the present (1860-2019). The HaNi dataset includes annual rates of synthetic N fertilizer, manure application/deposition, and atmospheric N deposition on cropland, pasture, and rangeland at a spatial resolution of 0.083°.

This project has received funding from the European Union's Horizon Europe research and innovation programme under grant agreement No 101081395

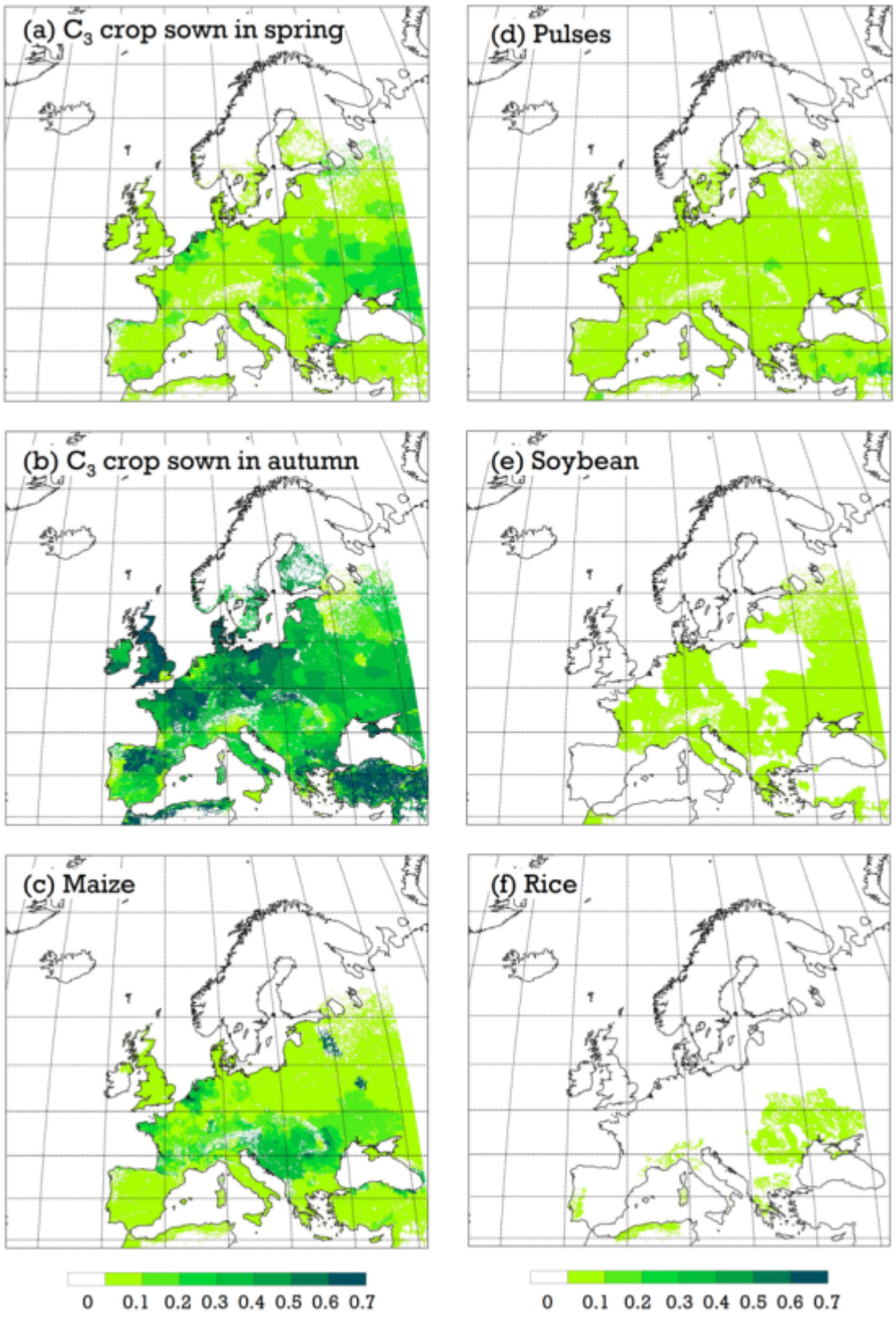

***Figure 10**: Maps of the rain-fed crop fractions, aggregated from MIRCA2000 crops to CFTs in LPJ-GUESS across Europe at 0.125° resolution.*

This project has received funding from the European Union's Horizon Europe research and innovation programme under grant agreement No 101081395

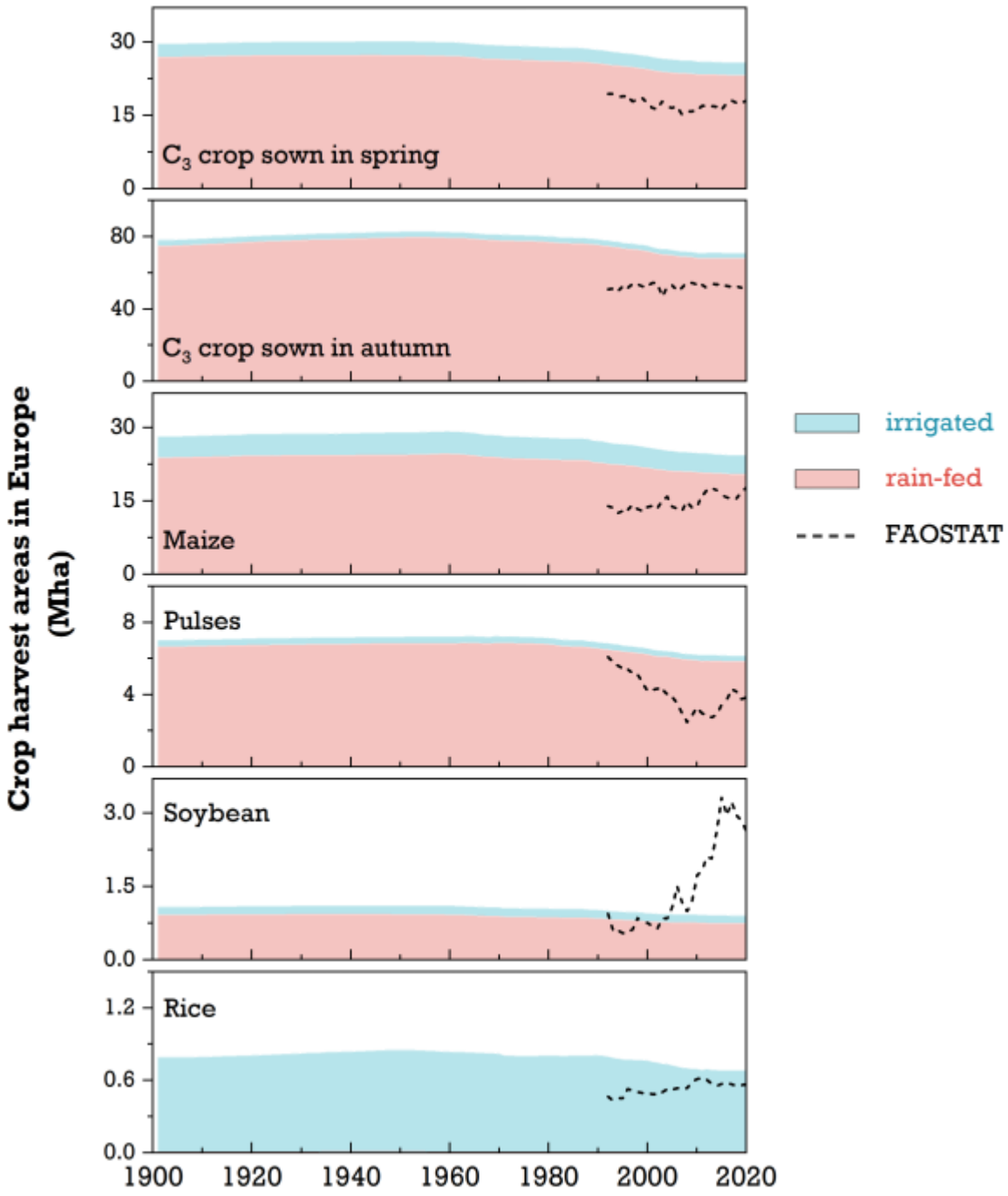

***Figure 11**: Simulated crop-specific total areas (rain-fed and irrigated; Mha) by combining HILDA+ with MIRCA2000 datasets over the historical period across Europe in LPJ-GUESS. The statistics from FAO between 1992-2020 used for comparison are shown in dashed lines*

This project has received funding from the European Union's Horizon Europe research and innovation programme under grant agreement No 101081395

We first aggregated the HaNi classes NH_4^+ and NO_3^- N fertilizer to the "synthetic N fertilizer" category from 0.083° to 0.125° resolution across European cropland and pasture (Table 6). Since the HaNi does not provide the crop-specific N input rates, we subsequently separated the total N application rates in each grid cell to each crop (Figure 12) using the crop fraction information from the MIRCA2000 dataset. Due to the unavailable information for the timing of N fertilizer application on a regional scale, we assumed with LPJ-GUESS that synthetic fertilizer application takes place at three crop development stages — sowing, halfway through the vegetative phase, and flowering — with different application rates depending on crop type. All manure is applied to crops at the time of sowing as a single application to reflect real-world practices that account for the time required for manure N to be made available to plants.

We compared the total N inputs from the HaNi with the statistics from FAO. Preliminary results indicate that our estimates of N fertilizer rates and manure application to agricultural soils in Europe are in general agreement with the FAO-based records in terms of both magnitude and long-term trends (Figure 13).

***Table 6**: Categorizing N input types from HaNi to LPJ-GUESS at 0.125° resolution in Europe*

N input classes in HaNi (from)	**N fertilization types in LPJ-GUESS (to)**
NH_4^+ N fertilizer in cropland	Synthetic N fertilizer in cropland
NO_3^- N fertilizer in cropland	
Manure application in cropland	Manure application in cropland
NH_4^+ N fertilizer in pasture	Synthetic N fertilizer in pasture
NO_3^- N fertilizer in pasture	
Manure application in pasture	N/A
Manure deposition in pasture	In the model, 25% of N in the harvested AGB on pasture is returned to the soils to simply account for the manure deposition from grazing animals
Manure deposition in rangeland	N/A

This project has received funding from the European Union's Horizon Europe research and innovation programme under grant agreement No 101081395

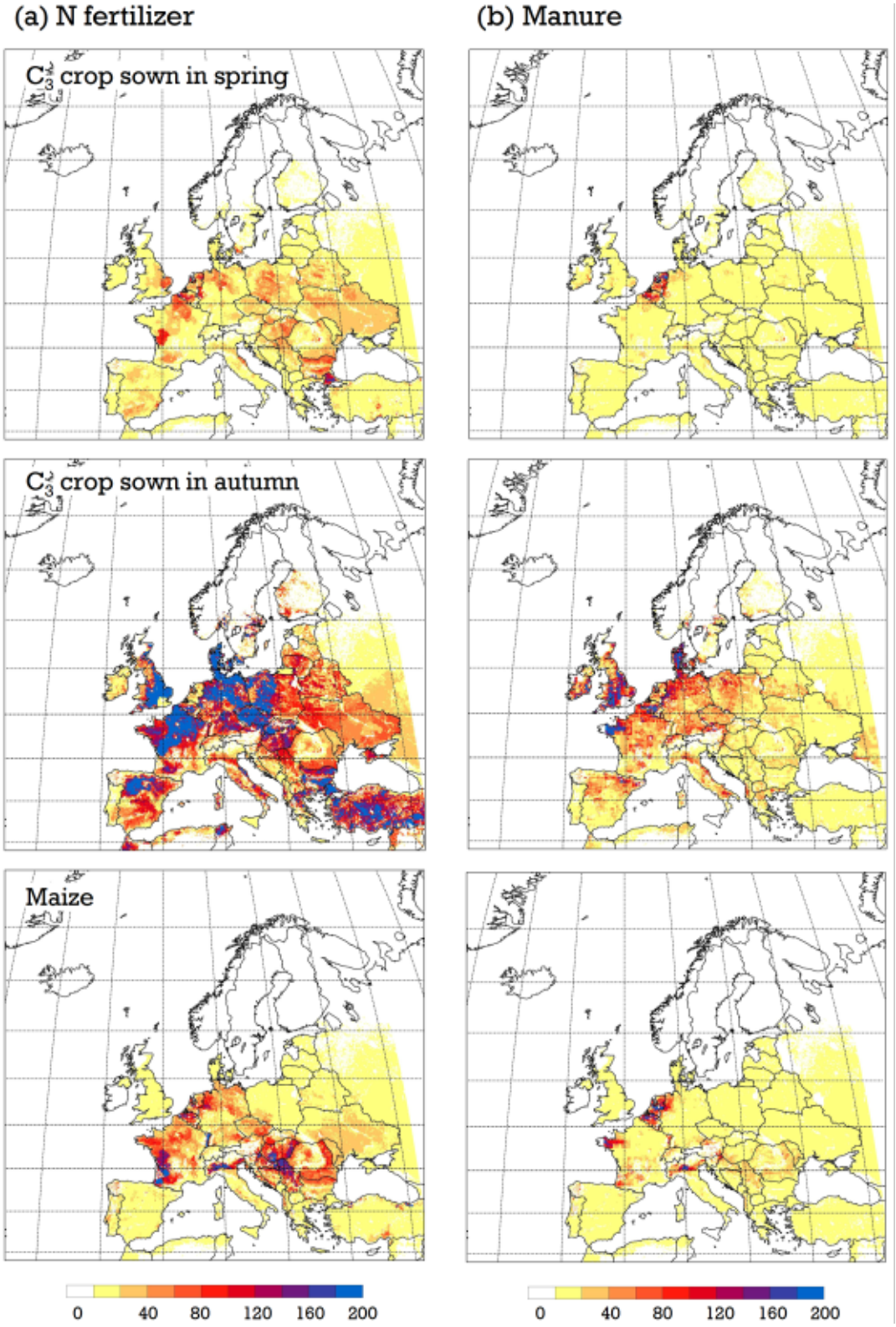

***Figure 12**: Maps of N fertilizer and manure applied to the three main crop types in Europe (tons N per grid cell averaged over 2010-2019), remapped from the HaNi dataset at 0.125° resolution for LPJ-GUESS.*

This project has received funding from the European Union's Horizon Europe research and innovation programme under grant agreement No 101081395

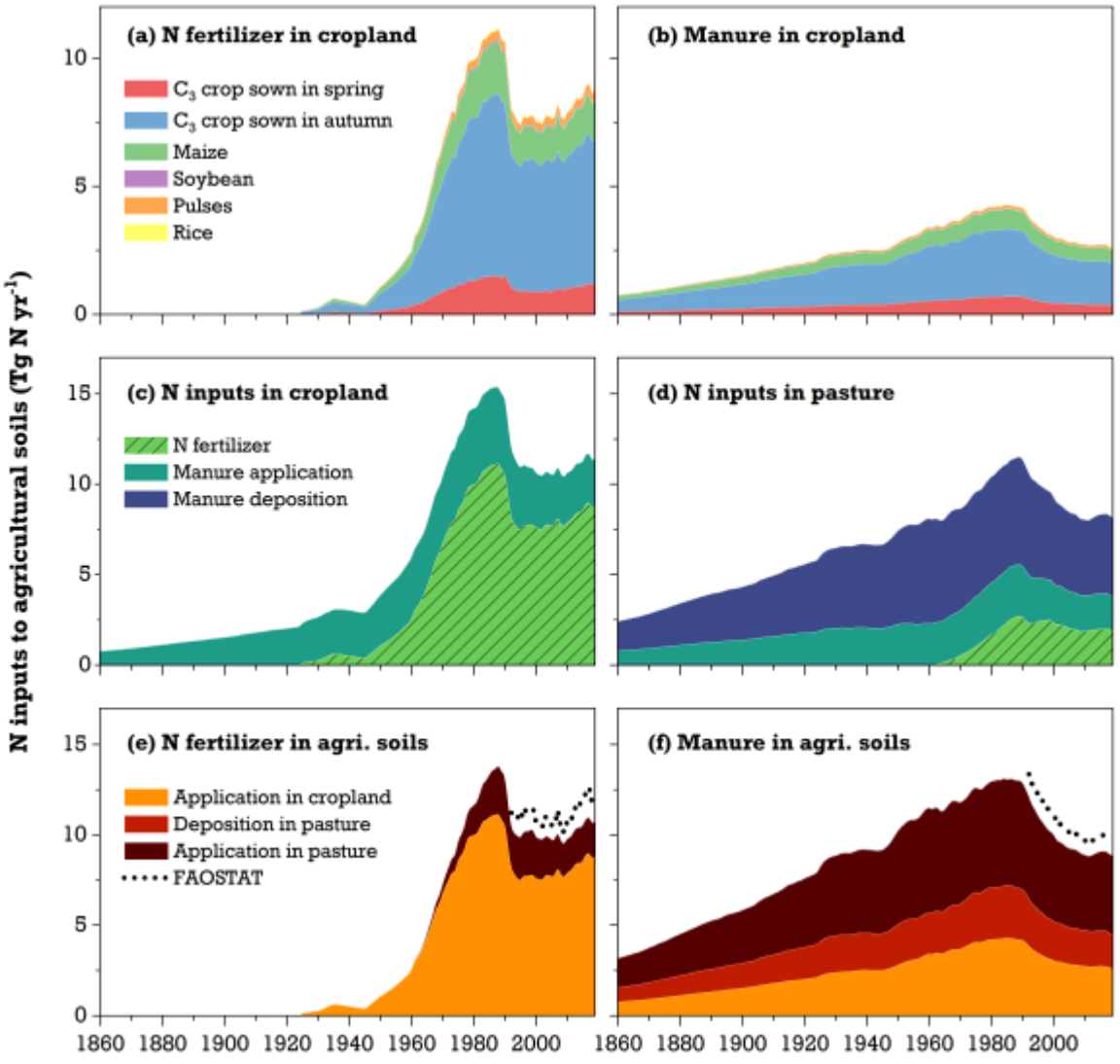

Figure 13: *The estimated total N inputs to cropland and pasture from the HaNi dataset between 1860 and 2019 across Europe. The statistics from FAO between 1992-2019 used for comparison are shown in dots.*

6. Grassland management datasets

In ORCHIDEE, there is a separate branch for grassland (as is the case for cropland) ORCHIDEE-GM (Grassland Management, Chang et al., 2013), that describes the impact of two grassland management practices (cutting and grazing) on grassland ecosystem dynamics and, in particular, on the exchange of carbon and water with the atmosphere. These developments were inspired (and partly taken) by a grassland model (PaSim, version 5.0). Current efforts are ongoing to integrate the grassland branch back into the main version of ORCHIDEE that includes the nitrogen cycle. In parallel, a second module was developed, CAMEO, in the ORCHIDEE model to describe the impact of agro-systems on the emission of ammonia and more generally on nitrogen transfers within agro-systems (Beaudor et al., 2023). Such module needs as main inputs the livestock density for each model grid cell.

In the second set of simulations, we still have not used the grassland management datasets, but as an update before the end of the project, the grassland management module and the agro-system module

This project has received funding from the European Union's Horizon Europe research and innovation programme under grant agreement No 101081395

will be activated. For these modules, we thus need the livestock distribution in Europe as livestock feeding and bedding needs are calculated within each grid cell from livestock density distribution maps, for different livestock categories. The distribution of each livestock category will be taken from the Gridded Livestock of the World dataset (GLW2; Robinson et al., 2014). This dataset can be accessed from the FAO website: https://www.fao.org/livestock-systems/en/. As an illustration, Figure 14 provides the distribution of cattle over the world, while 8 categories of livestock are reported in this dataset (Goats, Ducks, Buffaloes, Sheeps, Horses, Cattle, Pigs, and Chickens). From the livestock density in each grid cell, the grassland but also the cropland NPP will be used to provide the feeding and bedding needs (see Beaudor et al., 2023).

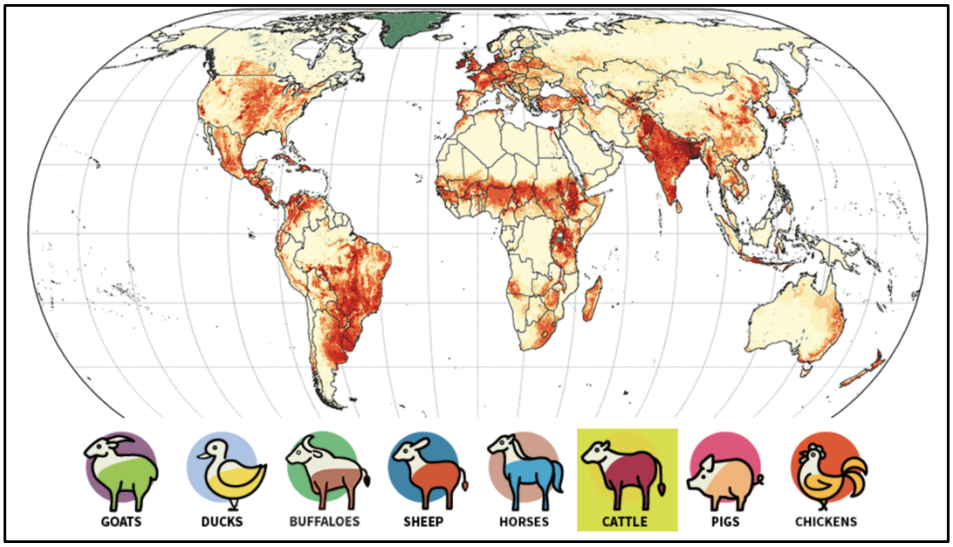

Figure 14: *Illustration of the Cattle global distribution from the FAO website: https://www.fao.org/livestock-systems/en/.*

In LPJ-GUESS, pasture is simulated with a uniform management intensity across all European grid cells. For instance, we assume that 50% of aboveground biomass is removed from pasture each year to broadly represent the effects of grazing. To parameterize internal manure deposition from livestock on grazing pastures, 75% of the harvested N from aboveground biomass is assumed to return to the soil annually. Given the widespread use of chemical N fertilizer on European agricultural soils, pasture receives a constant N application rate of 20 kg N ha^{-1} per year since 1990 (Tian et al., 2022).

For JSBACH, there is currently no specific need for grassland management data for the simulation of wetland CH_4 emissions.

7. Forest management datasets

For forests, ORCHIDEE and LPJ-GUESS are at different stages in terms of using forest management data. For ORCHIDEE, the second set of simulations planned for early 2025, will still not use the forest management module (diameter and age classes as well as tree height dynamics, described in Naudts et al., 2015) that has been only recently included in the trunk version of ORCHIDEE and coupled with the nitrogen cycle, given that some parameterisations are still under adjustment (mainly final adjustments for the mortality due to self-thinning intensity). Note that forest management in Europe significantly varies between countries and its description is thus difficult to parameterise given that many countries do not have clear-felling but rather complex thinning practices. However, such a demography-based version will be used for the CMIP7-FastTrack exercise at the end of 2025, and we will thus be able to

This project has received funding from the European Union's Horizon Europe research and innovation programme under grant agreement No 101081395

provide an updated ORCHIDEE run for the EYE-CLIMA GHG synthesis (WP4). In this context, we have gathered different datasets that are currently used for ORCHIDEE calibration and evaluation or that will be used in the next round of simulation directly as inputs. First, we are trying to valorise in-situ data that were produced and collected during various projects and, in particular, the VERIFY precursor project, through a dedicated activity on forest data collection. Second, we are trying to use spatial products, combining in situ and remote sensing observations, as described for example in Pucher et al. (2022).

For LPJ-GUESS, clear-cutting harvest is applied to managed forest ecosystems to match present-day forest age structure described in Pucher et al. (2022). Following a clear-cut event, all tree species in the regrowth phase undergo a fixed thinning intensity, determined based on Reineke's self-thinning rules, where trees of all sizes and ages are cut equally. To prevent tree mortality caused by the model's self-thinning functionality, we assume that these forests are managed under extensive thinning practices (the model's default setup), with the target relative density index set at 0.85 in the simulations. This index is defined as the ratio of tree density and maximum density, where higher values indicate lower thinning intensity (Lindeskog et al., 2021). Thinning may be triggered when tree density reaches the target relative density index.

7.1 In situ forest datasets

We first choose to valorise the data collected during the previous EU project, VERIFY, that had also a specific focus on European greenhouse gas budgets. The data have not been transferred to the EYE-CLIMA data portal, but they are taken directly from the VERIFY database (https://webportals.ipsl.fr/VERIFY/Ressources_2D.html). For a detailed description of the different datasets, we refer to specific VERIFY deliverable that are accessible from: https://verify.lsce.ipsl.fr/index.php/repository/public-deliverables/wp3-verification-methods-for-terrestrial-co2-sources-and-sinks-and-carbon-stock. We thus provide below a brief note on these products.

In-situ National Forest Inventory (NFI) data

More and more countries in Europe are setting up NFI programmes, where especially Central/Eastern European countries are changing from inventories based on Forest Management Planning systems towards statistically based NFI programmes. However, NFI data are considered politically sensitive, and in-situ plot data are not always shared. Gradually, this attitude is changing with more and more countries publishing their raw data on the internet or making them available on request for specific purposes and projects. Figure 15 illustrates the location of the different NFI data that were collected; there is a clear gradient of decreasing availability of raw NFI data from West to East in Europe. The collected raw data are thus available to both ORCHIDEE and LPJ-GUESS teams to evaluate, for example, the simulated height, diameter, and volume increments.

This project has received funding from the European Union's Horizon Europe research and innovation programme under grant agreement No 101081395

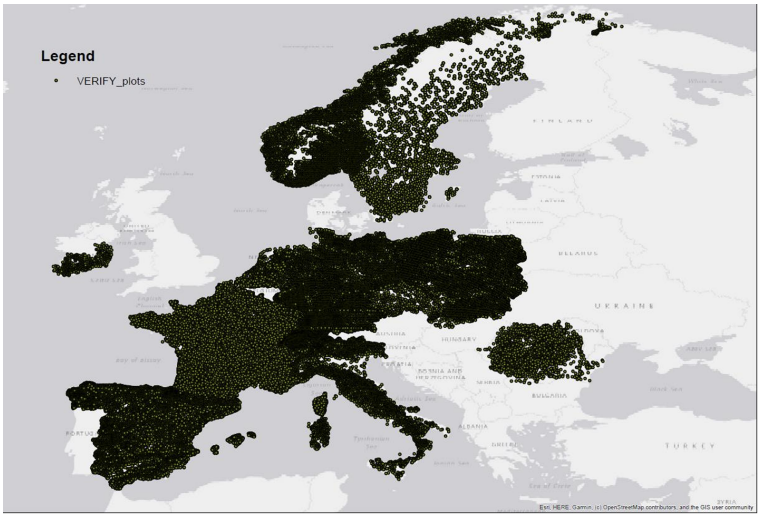

Figure 15: *Availability of raw NFI data over Europe gathered in VERIFY project (see https://verify.lsce.ipsl.fr/index.php/repository/public-deliverables/wp3-verification-methods-for-terrestrial-co2-sources-and-sinks-and-carbon-stock/d3-14-national-forest-inventory-and-high-resolution-forest-cover-for-eastern-europe).*

Observed management and mortality data

Observed mortality due to management or natural causes based on NFI data is provided in Schelhaas et al. (2018a,b). The most important species are treated individually, while the remainder are combined into one group. Data are presented by 5 cm classes, separately for management (HarvestProbability) and natural causes (DeadProbability) (see Figure 16). Note that harvested trees will include trees that died for natural reasons and that were subsequently extracted. These data are being used by the modelling groups to define spatially explicit forest management intensity.

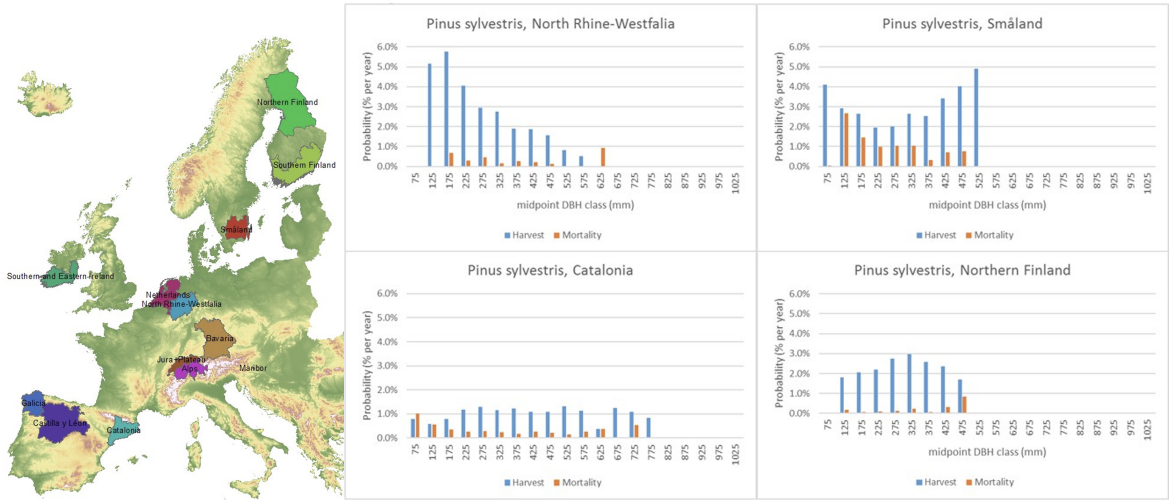

Figure 16: *Left: regions for which management and mortality data are provided; Right: Example of regionally different patterns of management and mortality in Pinus sylvestris (Schelhaas et al., 2018b)*

This project has received funding from the European Union's Horizon Europe research and innovation programme under grant agreement No 101081395

Biomass – age relationships

To evaluate the performance of the models in simulating biomass-age relationship, an age - biomass evaluation dataset of plot-scale forest type and forest biomass was specifically constructed for ORCHIDEE by integrating several existing databases. The work was done by the main contributors of the forest demography developers of ORCHIDEE, namely, S. Luyssaert, G. Marie, Yue Chao and Pengyi Zhang; the dataset includes:

1. the Forest Carbon Database (ForC) (Anderson-Teixeira et al., 2021)
2. the forest biomass structure dataset for Eurasia (Schepaschenko D et al., 2017)
3. a fieldwork database established by Zhu et al. (2017).
4. chronosequence-based dataset collected by Ye et al. (2021) (Note that this chronosequence database is to be published).
5. a fieldwork database collected by Luo et al., (2018)
6. a dataset from Poorter et al. (2017)

These existing databases provide information on geographic location (latitude and longitude), dominant species or forest types, stand age, and aboveground or belowground biomass or total biomass carbon stock. It should be noted that sites in the ForC dataset may consist of multiple different plots. Following this procedure and to ensure the consistency of the constructed database, the leaf forms were divided into needleleaf and broadleaf, the leaf types into deciduous and evergreen, and the climates into tropical, temperate and boreal forest, according to the information on dominant species. In addition, biomass density (Mg ha-1) was converted to biomass carbon density (g C m-2) using the conversion factor of 0.47. The above processing generated a database containing information on geographic location, forest types, leaf forms, leaf types, stand age, and aboveground or belowground biomass carbon density. These data are currently being used directly by the ORCHIDEE group to calibrate the regrowth curves of the ORCHIDEE – V4 version (including forest demography). Figure 17 below illustrates the location of the points that were collected.

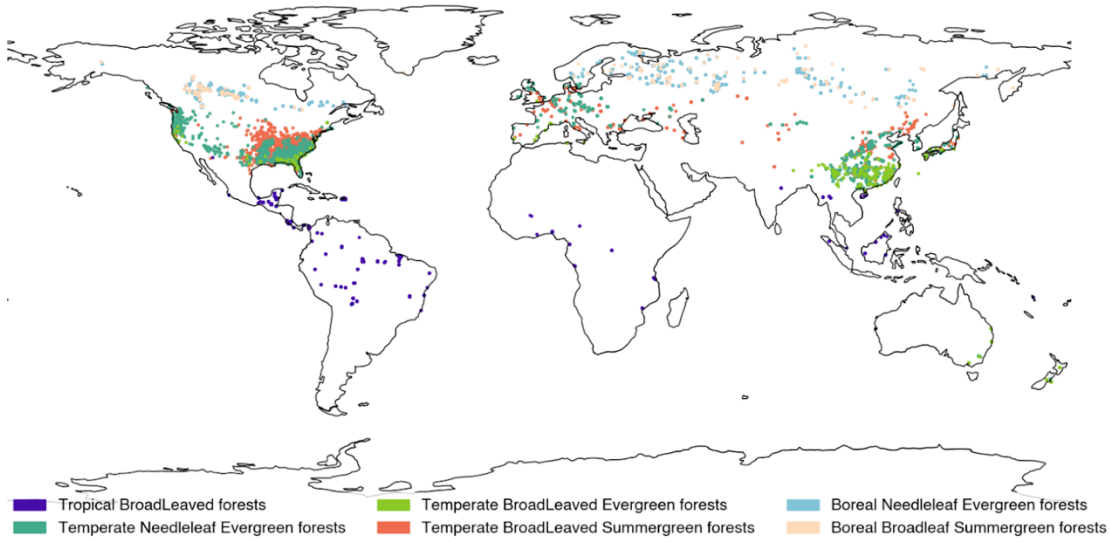

Figure 17: *Spatial distribution of the observation sites compiled to calibrate the age-biomass regrowth curves of the ORCHIDEE model.*

This project has received funding from the European Union's Horizon Europe research and innovation programme under grant agreement No 101081395

7.2 Remote sensing derived forest datasets

Estimates of forest above-ground biomass and carbon changes (ΔAGB/C) using remote sensing have progressed due to the increasing demand from the scientific community and countries, in line with the increasing availability of satellite data. Recently, several methods and maps of forest carbon fluxes have been published using the "spatial approach" of mapping ΔAGB/C in multiple periods. Harris et al. (2021) mapped carbon fluxes using forest "gain-loss" pixels (Hansen et al., 2013), where the gained or lost carbon is estimated separately depending on the nature of changes from the IPCC activity data. Other recent methods used spaceborne radar and LiDAR data to map AGB/C in multiple periods (ESA-CCI product, Santoro and Cartus, 2021) and in time series (JPL product, Xu et al., 2021).

The data from these studies were used to assess carbon fluxes for Europe from 2010 to 2018 during the VERIFY project. All products were adjusted for bias using independent reference biomass datasets following the uncertainty assessment framework in Araza et al. (2022). In total, six map-based estimates of forest carbon fluxes were derived that were also compared with the estimates from the Forest Resource Assessment (FRA). FRA data are available for the years 2010, 2015, and 2020 so they averaged 2015 and 2020 to obtain a 2018 proxy.

More details on these products are available in the report:

https://verify.lsce.ipsl.fr/index.php/repository/public-deliverables/wp3-verification-methods-for-terrestrial-co2-sources-and-sinks-and-carbon-stock/d3-14-national-forest-inventory-and-high-resolution-forest-cover-for-eastern-europe

Part of these data are currently being used for the evaluation of the ORCHIDEE model outputs, and some datasets were revised according to recent updates. In particular, we are currently mainly using the above ground biomass data from the ESA-CCI project and especially the most recent version V5, covering the period 2010 – 2021. Figure 18 illustrates the distribution of the above ground biomass of the ESA product that we are currently using to evaluate the biomass distribution of ORCHIDEE.

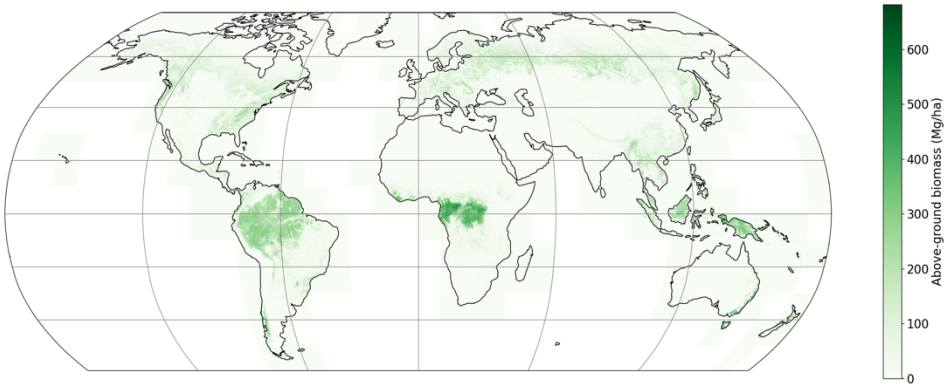

Figure 18: *Illustration of the above ground biomass distribution from the ESA-CCI biomass dataset (V5): https://climate.esa.int/en/projects/biomass/.*

Pucher dataset

Pucher et al. (2022) released a recent dataset to provide an improved forest structure for Europe. Harmonized inventory data from 16 European countries were used in combination with remote sensing data and a gap-filling algorithm to produce a consistent and comparable forest structure dataset across European forests. They showed how land cover data can be used to scale inventory data to a higher

This project has received funding from the European Union's Horizon Europe research and innovation programme under grant agreement No 101081395

resolution, which in turn ensures a consistent data structure across sub-national, country and European forest assessments. Cross-validation and comparison with published country statistics of the Food and Agriculture Organization (FAO) indicated that their methodology was able to produce robust and accurate forest structure data across Europe, even for areas where no inventory data were available.

Such dataset is available from the BOKU university in Vienna: https://boku.ac.at/en/wabo/waldbau/wir-ueber-uns/daten and will be used separately by the LPJ-GUESS and ORCHIDEE teams. The dataset comprises several variables of interest for both groups, including volume, carbon content, biomass by compartment, height, diameter at breast height, stem number, basal area, stand density index, age class and tree species group. Figure 19 illustrates the two main variables (age class and tree height) that we are currently using to constraint our model. Indeed, one key challenge is to have some coherence between the land cover change/use products, the management rule implemented in the models and the age specified in the Pucher dataset.

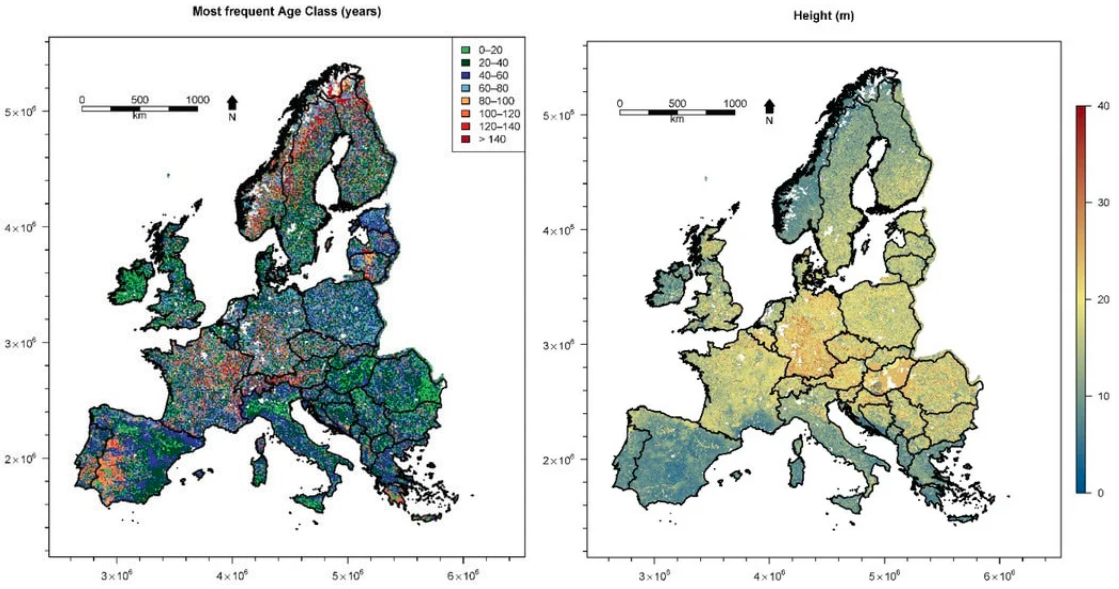

Figure 19: *Illustration of the most frequent age class (left map; in years) and the tree height (right map, in metres) from Pucher et al., (2022) dataset. The data are gridded on an 8 × 8 km cell. Note that within each cell no distinction between forested or non-forested area is made; and a forest area mask is needed to quantify extent of forests.*

8. Conclusion

This deliverable presents key datasets that are either currently being used as inputs for the ongoing model simulations of CO_2, CH_4 and N_2O fluxes or used as validation and calibration for the development of the three models involved in EYE-CLIMA: ORCHIDEE, LPJ-GUESS and JSBACH. The EYE-CLIMA model input datasets deliverable has grown out of a collaboration between the three modelling groups. As such, the collection of data and development of model inputs will continue as user needs evolve. This is the second and final release of the deliverable.

This project has received funding from the European Union's Horizon Europe research and innovation programme under grant agreement No 101081395

9. References

Anderson-Teixeira, K. J., Herrmann, V., Morgan, R. B., Bond-Lamberty, B., Cook-Patton, S. C., Ferson, A. E., ...& Wang, M. M. (2021). Carbon cycling in mature and regrowth forests globally. Environmental Research Letters, 16(5), 053009.

Araza, A., de Bruin, S., Herold, M., Quegan, S., Labriere, N., Rodriguez-Veiga, P., Avitabile, V., Santoro, M., Mitchard, E.T.A., Ryan, C.M., Phillips, O.L., Willcock, S., Verbeeck, H., Carreiras, J., Hein, L., Schelhaas, M.-J., Pacheco-Pascagaza, A.M., da Conceição Bispo, P., Laurin, G.V., Vieilledent, G., Slik, F., Wijaya, A., Lewis, S.L., Morel, A., Liang, J., Sukhdeo, H., Schepaschenko, D., Cavlovic, J., Gilani, H., Lucas, R., 2022. A comprehensive framework for assessing the accuracy and uncertainty of global above-ground biomass maps. Remote Sensing of Environment 272, 112917. https://doi.org/10.1016/j.rse.2022.112917

Ballabio C., Panagos P., Montanarella L. Mapping topsoil physical properties at European scale using the LUCAS database (2016) Geoderma, 261 , pp. 110-123.

Beaudor, M., Vuichard, N., Lathière, J., Evangeliou, N., Van Damme, M., Clarisse, L., and Hauglustaine, D.: Global agricultural ammonia emissions simulated with the ORCHIDEE land surface model, Geosci. Model Dev., 16, 1053–1081, https://doi.org/10.5194/gmd-16-1053-2023, 2023.

Chang, J.F., Viovy, N., Vuichard, N., Ciais, P., Wang, T., Cozic, A., Lardy, R., Graux, A.I., Klumpp, K., Martin, R. and Soussana, J.F., 2013. Incorporating grassland management in ORCHIDEE: model description and evaluation at 11 eddy-covariance sites in Europe. Geoscientific Model Development, 6(6), pp.2165-2181.

FAO & IIASA. 2023. Harmonized World Soil Database Version 2.0. Rome and Laxenburg, https://doi.org/10.4060/cc3823en

FAOSTAT. (2023). Production/Crops and livestock products [dataset]. Retrieved from https://www.fao.org/faostat/en/#data

Fluet-Chouinard, E., Stocker, B.D., Zhang, Z. et al. Extensive global wetland loss over the past three centuries. Nature 614, 281–286 (2023). https://doi.org/10.1038/s41586-022-05572-6

Hagemann, S., Stacke, T., 2015. Impact of the soil hydrology scheme on simulated soil moisture memory. Clim Dyn 44, 1731–1750. https://doi.org/10.1007/s00382-014-2221-6

Harris, N. L., Gibbs, D. A., Baccini, A., Birdsey, R. A., De Bruin, S., Farina, M., ... & Tyukavina, A. (2021). Global maps of twenty-first century forest carbon fluxes. Nature Climate Change, 11(3), 234-240.

Hansen, M. C., Potapov, P. V., Moore, R., Hancher, M., Turubanova, S. A., Tyukavina, A., ... & Townshend, J. (2013). High-resolution global maps of 21st-century forest cover change. science, 342(6160), 850-853.

Lehner, B., Anand, M., Fluet-Chouinard, E., Tan, F., Aires, F., Allen, G. H., Bousquet, P., Canadell, J. G., Davidson, N., Finlayson, C. M., Gumbricht, T., Hilarides, L., Hugelius, G., Jackson, R. B., Korver, M. C., McIntyre, P. B., Nagy, S., Olefeldt, D., Pavelsky, T. M., Pekel, J.-F., Poulter, B., Prigent, C., Wang, J., Worthington, T. A., Yamazaki, D., and Thieme, M.: Mapping the world's inland surface waters: an update to the Global Lakes and Wetlands Database (GLWD v2), Earth Syst. Sci. Data Discuss. [preprint], https://doi.org/10.5194/essd-2024-204, in review, 2024.

Lindeskog, M., Smith, B., Lagergren, F., Sycheva, E., Ficko, A., Pretzsch, H., & Rammig, A. (2021). Accounting for forest management in the estimation of forest carbon balance using the dynamic vegetation model LPJ-GUESS (v4.0, r9710): Implementation and evaluation of simulations for Europe. Geoscientific Model Development (Vol. 14). https://doi.org/10.5194/gmd-14-6071-2021

This project has received funding from the European Union's Horizon Europe research and innovation programme under grant agreement No 101081395

Luo, Y., Chen, H. Y., McIntire, E. J., & Andison, D. W. (2021). Data from: Divergent temporal trends of net biomass change in western Canadian boreal forests.

Ministry of Environment (2023), Report on Monitoring and State of Finland's Soil and Policy Instruments for its Use (editor: T. Haavisto), Publications of the Ministry of Environment 2023:33, 257 pages, https://urn.fi/URN:ISBN:978-952-361-578-6

Naudts, K., Ryder, J., McGrath, M. J., Otto, J., Chen, Y., Valade, A., ... & Luyssaert, S. (2015). A vertically discretised canopy description for ORCHIDEE (SVN r2290) and the modifications to the energy, water and carbon fluxes. Geoscientific Model Development, 8(7), 2035-2065.

Poggio, L., De Sousa, L. M., Batjes, N. H., Heuvelink, G., Kempen, B., Ribeiro, E., & Rossiter, D. (2021). SoilGrids 2.0: producing soil information for the globe with quantified spatial uncertainty. Soil, 7(1), 217-240.

Poorter, L., Bongers, F., Aide, T. M., Almeyda Zambrano, A. M., Balvanera, P., Becknell, J. M., ... & Rozendaal, D. (2016). Data from: Biomass resilience of Neotropical secondary forests. Dryad, Dataset, 10.

Portmann, F. T., Siebert, S., & Döll, P. (2010). MIRCA2000-Global monthly irrigated and rainfed crop areas around the year 2000: A new high-resolution dataset for agricultural and hydrological modeling. Global Biogeochemical Cycles, 24(1), 1–24. https://doi.org/10.1029/2008gb003435

Pucher, C., Neumann, M., & Hasenauer, H. (2022). An Improved Forest Structure dataset for Europe. Remote Sensing, 14(2), 395.

Ribeiro, E., & Batjes, N. (2019, January). WoSIS: standardised soil profile data for digital soil mapping at global scale. In Geophysical Research Abstracts (Vol. 21).

Robinson TP, Wint GRW, Conchedda G, Van Boeckel TP, Ercoli V, Palamara E, Cinardi G, DâAietti L, Hay SI, and Gilbert M. (2014) Mapping the Global Distribution of Livestock. PLoS ONE 9(5): e96084. doi:10.1371/journal.pone.0096084

Santoro, M., Cartus, O., Carvalhais, N., Rozendaal, D., Avitabile, V., Araza, A., ... & Willcock, S. (2021). The global forest above-ground biomass pool for 2010 estimated from high-resolution satellite observations. Earth System Science Data, 13(8), 3927-3950.

Santoro, M., & Cartus, O. (2021). ESA biomass climate change initiative (Biomass_cci): Global datasets of forest above-ground biomass for the years 2010, 2017 and 2018, v3. Cent. Environ. Data Anal.

Schelhaas MJ, Hengeveld GM, Heidema N, Thürig E, Rohner B, Vacchiano G, Vayreda J, Redmond J, Socha J, Fridman J, Tomter S, Polley H, Barreiro S, Nabuurs GJ, 2018a. Species-specific, pan-European diameter increment models based on data of 2.3 million trees. Forest Ecosystems 5:21 doi.org/10.1186/s40663018-0133-3

Schelhaas MJ, Fridman J, Hengeveld GM, Henttonen H, Lehtonen A, Kies U, Krajnc N, Lerink B, Ní Dhubháin A, Polley H, Pugh TAM, Redmond J, Rohner B, Temperli C, Vayreda J, Nabuurs GJ, 2018b. Actual European forest management by region, tree species and owner based on 714,000 re-measured trees in national forest inventories. PLoS ONE 13(11): e0207151.

Schepaschenko, D., Shvidenko, A., Usoltsev, V., Lakyda, P., Luo, Y., Vasylyshyn, R., ... & Obersteiner, M. (2017). A dataset of forest biomass structure for Eurasia. Scientific data, 4(1), 1-11.

Still, C.J., Cotton, J.M., Griffith, D.M., 2019. Assessing earth system model predictions of C4 grass cover in North America: From the glacial era to the end of this century. Global Ecology and Biogeography 28, 145–157.

Tanneberger, F., Tegetmeyer, C., Busse, S., Barthelmes, A., and 55 others, 2017. The peatland map of Europe. Mires and Peat 1–17. https://doi.org/10.19189/MaP.2016.OMB.264

This project has received funding from the European Union's Horizon Europe research and innovation programme under grant agreement No 101081395

Tian, H., Bian, Z., Shi, H., Qin, X., Pan, N., Lu, C., et al. (2022). History of anthropogenic Nitrogen inputs (HaNi) to the terrestrial biosphere: a 5 arcmin resolution annual dataset from 1860 to 2019. Earth System Science Data, 14(10), 4551–4568. https://doi.org/10.5194/essd-14-4551-2022

Winkler, K., Fuchs, R., Rounsevell, M. D., & Herold, M. (2020). HILDA+ Global Land Use Change between 1960 and 2019. Pangaea https://doi. org/10.1594/PANGAEA, 921846.

Wu, X., Vuichard, N., Ciais, P., Viovy, N., de Noblet-Ducoudré, N., Wang, X., ... & Ripoche, D. (2016). ORCHIDEE-CROP (v0), a new process-based agro-land surface model: model description and evaluation over Europe. Geoscientific Model Development, 9(2), 857-873.

Xu, J., Morris, P.J., Liu, J. and Holden, J. (2018). PEATMAP: Refining estimates of global peatland distribution based on a meta-analysis, CATENA, 160, 134-140, https://doi.org/10.1016/j.catena.2017.09.010

Xu, L., Saatchi, S. S., Yang, Y., Yu, Y., Pongratz, J., Bloom, A. A., ... & Schimel, D. (2021). Changes in global terrestrial live biomass over the 21st century. Science Advances, 7(27), eabe9829.

Ye, J., Yue, C., Hu, Y., & Ma, H. (2021). Spatial patterns of global-scale forest root-shoot ratio and their controlling factors. Science of the Total Environment, 800, 149251.

Zhang, Z., Fluet-Chouinard, E., Jensen, K., McDonald, K., Hugelius, G., Gumbricht, T., Carroll, M., Prigent, C., Bartsch, A., and Poulter, B.: Development of the global dataset of Wetland Area and Dynamics for Methane Modeling (WAD2M) , Earth Syst. Sci. Data, 13, 2001–2023, https://doi.org/10.5194/essd-13-2001-2021, 2021.

Zhu, J., Hu, H., Tao, S., Chi, X., Li, P., Jiang, L., ... & Fang, J. (2017). Carbon stocks and changes of dead organic matter in China's forests. Nature Communications, 8(1), 151.

This project has received funding from the European Union's Horizon Europe research and innovation programme under grant agreement No 101081395

https://eyeclima.eu

BRUSSELS, 17 04 2025

Funded by the European Union. Views and opinions expressed are however those of the author(s) only and do not necessarily reflect those of the European Union. Neither the European Union nor the granting authority can be held responsible for them.

This project has received funding from the European Union's Horizon Europe research and innovation programme under grant agreement No 101081395